

MICROSTRUCTURAL EFFECTS ON THE LUMINESCENCE INTENSITY OF Pr³⁺-DOPED CaTiO₃

PHILIPPE BOUTINAUD, ERIC PINEL, GENEVIÈVE BERTRAND, RACHID MAHIOU, PETRA JAKUBCOVÁ*, STANISLAV KASA*

*Laboratoire des Matériaux Inorganiques - UMR CNRS 6002. Université Blaise-Pascal et ENSCCF
Ensemble Scientifique des Cèzeaux, 63177 Aubiere Cedex, France
E-mail: boutinau@chimtp.univ-bpclermont.fr*

**Department of Glass and Ceramics
Institute of Chemical Technology, Prague, Technická 5, 166 28 Prague, Czech Republic
E-mail: Stanislav.Kasa@vscht.cz*

Submitted March 27, 2002; accepted July 12, 2002

Keywords: CaTiO₃, Luminescence, Microstructure, Praseodymium

The microstructural and luminescence characteristics of solid state (SS) and sol-gel (SG) processed CaTiO₃:Pr³⁺ powders have been investigated as a function of the grinding time t , in the case of SS, samples and of OH/Ti(OPr)₄ molar ratios r , in the case of SG, samples. It is observed that either extended post-synthesis grinding or sol-gel syntheses operated under acid or neutral conditions lead to submicron grained microstructures, CaTiO₃ + TiO₂ phase mixing and finally to less efficient phosphors. The observed decrease of luminescence intensity is correlated to the presence of non-luminescent rutile and to the amount of submicron particles.

INTRODUCTION

Pr³⁺-doped calcium titanate is known for several years as a red emitting phosphor characterized by a single emission peak with chromaticity coordinates positioned at $x = 0.68$, $y = 0.311$, very close to the ones of the "ideal red", as their are defined by the CIE (Commission Internationale de l'Eclairage) [1]. Although this material has been reported in 1994 as an attractive phosphor for low voltage field emission displays [2], no investigation, to our knowledge, has been further undertaken to improve its brightness. However, in a recent work [3], significant reinforcement of the red luminescence intensity in Pr³⁺-doped calcium titanate powders has been demonstrated by preparing these phosphors by sol-gel procedure under basic conditions and by adjusting the stoichiometry with appropriate charge compensators. In this study, the influence of the sintering conditions on the optical performance have also been carefully analyzed, since the temperature and the duration of the thermal treatments are known to affect strongly the degree of crystallization and the densification of the powders. Here, we report on an investigation of microstructural effects, including grains size repartition, on the optical performance of Pr³⁺-doped calcium deficient titanates with nominal formula Ca_{(1-3x/2)#x/2}Pr_xTiO₃ and $x = 0.2$ %. In this material, $x/2$ formula units of Ca vacancies (denoted #) are created per formula units of Pr³⁺ for charge compensation purposes. The materials

have been prepared either by solid state reaction or by the sol-gel route, using anhydrous CaCl₂, PrCl₃ and Ti isopropoxide in isopropanol and aqueous NH₄OH as the base (see details of the protocol in [3]). Whatever the synthesis method, the sintering conditions were kept identical at 1200 °C for 4 hours under air. Modulation of the microstructure (especially particle size and its distribution) was operated either mechanically by grinding the solid state processed powders for different times ranging from 5 to 75 minutes or, without grinding, by varying the pH of the gel during the sol-gel procedure. In this latter case, the different investigated OH/Ti(OPr)₄ molar ratios were respectively $r = 0.39$, 0.78, 8.5, 12.7 and 17. The corresponding samples will be denoted SGr in the following, by reference to the values of the molar ratios. For all these syntheses, water was in excess, to ensure appropriate conditions for total hydrolysis of the Ti(OPr)₄ groups. However, the hydrolysis-condensation process can be strongly influenced by the OH/Ti(OPr)₄ molar ratio, as described for example in [4]. Accordingly, when $r \gg 2$ (pH maintained in a range from 11 to 14), a nucleophilic attack of Ti(OPr)₄ by OH-groups can be involved, yielding Ti(OH)₆²⁻ anions following the equation: Ti(OPr)₄ + 4 H₂O + 2 OH⁻ → Ti(OH)₆²⁻ + 4 HOPr. These anions, which contain six-fold coordinated Ti⁴⁺ ions as in the final perovskite network, are then neutralized by Ca²⁺ cations by internal condensation and release of water, forming appropriate precursors for the CaTiO₃ structure.

EXPERIMENTAL

The solid state processed powders have been crushed in a 50 ml agate mill pot with a total of 10 agate balls of 10-mm diameter, by using a Retsch S100 grinder operated at 500 rpm. The corresponding samples will be denoted respectively SS_t , where the subscript t indicates the grinding time in minutes. In addition, two samples denoted $SS_{15}(>5 \mu\text{m})$ and $SS_{15}(<5 \mu\text{m})$ have been obtained by sifting a SS_{15} sample on a $5 \mu\text{m}$ sieve. The structural properties of the materials, before and after milling, were controlled systematically by X-ray diffraction, using a Siemens D5000 diffractometer equipped with Cu anode operated at 40 kV and 30 mA. The microstructural characteristics were checked either by scanning electron microscopy (SEM) (Cambridge Scan 360) operated at 10 kV or by laser granulometry (Mastersizer, Malvern Instruments). In the case of this latter technique, anionic surfactant and distilled water were used as dispersant and the ultrasonic treatment was fixed at 15 minutes for all samples. The optical measurements of the photoluminescence intensity were carried out at room temperature by using the 345 nm monochromatized radiation supplied by a 250 Watt CW xenon lamp and a computer-controlled Bausch & Lomb double grating monochromator equipped with a EMI 9698 QB photomultiplier, as a detector. The intensity was evaluated by integrating the red emission band in a range from 600 to 650 nm. For comparison purposes, special care was taken to control the beam power of the excitation source and to keep identical the illuminated surface of the sample.

RESULTS AND DISCUSSION

X-ray powder diffraction

Typical X-ray diffraction (XRD) patterns of SS_t and SG_r samples are displayed in figure 1 and 2, respectively. While the pattern of SS_0 is characteristic of single-phased orthorhombic CaTiO_3 , the patterns of SS_t samples with $t > 0$ clearly show $\text{CaTiO}_3 + \text{TiO}_2$ phase mixing with increasing amount of rutile TiO_2 , as t is increased. The patterns of the two sifted samples $SS_{15}(>5 \mu\text{m})$

and $SS_{15}(<5 \mu\text{m})$ confirm the presence of residual rutile in both samples. Concerning SG_r samples, the XRD patterns exhibit also $\text{CaTiO}_3 + \text{TiO}_2$ phase mixing, but only for the lowest values of r , corresponding to acid or neutral synthesis conditions. The presence of residual CaO is never detected. The samples prepared under basic conditions are single phased.

Laser granulometry

The granulometric characteristics of the solid state titanates SS_t and sol-gel processed titanates SG_r are gathered in table 1. The parameters $D(\text{av})$, $D(0.9)$ and $\% (D < 1 \mu\text{m})$ were selected since they provide a global representativity of the microstructure of the powders: $D(\text{av})$ represents the average particle size for particles larger than $1 \mu\text{m}$, $D(0.9)$ is the size for which 90 % of the particles have a diameter smaller than the value and $\% (D < 1 \mu\text{m})$ represents the volumetric percentage of submicron particles dissociated by the ultrasonic treatment. For all the tested powders, the particle size distribution is either monomodal or bimodal, depending on the t or r values. In the case of SS_t samples, the particles distribution is monomodal only for $t = 0$ min (unground sample). As the grinding time is increased, the granulometric profiles are shifted to lower particles size values and present a shoulder in the submicrometer region. The volumic proportion of these submicron particles increases gradually as t is increased, while concomitantly, $D(\text{av})$ and $D(0.9)$ decrease in a way such that it leads to a narrowing of the particle size distribution for particles larger than $1 \mu\text{m}$. The effect of sifting can be analysed by comparing SS_{15} , $SS_{15}(>5 \mu\text{m})$ and $SS_{15}(<5 \mu\text{m})$ samples. As expected, all the submicron particles evidenced in unsifted SS_{15} appear in $SS_{15}(<5 \mu\text{m})$, which presents therefore a bimodal distribution, while $SS_{15}(>5 \mu\text{m})$ sample is characterized by a narrow monomodal distribution of particles larger than $1 \mu\text{m}$, with an average size of about $20 \mu\text{m}$. In $SS_{15}(<5 \mu\text{m})$, particles as large as $9 \mu\text{m}$ are detected (see table 1) suggesting a tendency for the smallest particles to re-aggregate. For uncrushed SG_r samples, the granulometric parameters appear to be strongly dependent on the value of r . Under acidic conditions ($r = 0.39$), the powder is made up of a

Table 1. Granulometric parameters and luminescence intensity of SS_t and SG_r samples.

	$a-SS_0$	$a-SS_5$	$a-SS_{15}$	$a-SS_{35}$	$a-SS_{75}$	$a-SS_{15}>5 \mu\text{m}$	$a-SS_{15}<5 \mu\text{m}$	$SG_{0.39}$	$SG_{0.78}$	$SG_{8.5}$	$SG_{12.7}$	SG_{17}
$D(\text{av}) (\mu\text{m})$	30	10	4	3	2	10	5	200	22	25	30	35
$D(0.9) (\mu\text{m})$	47	28	10	4	3	20	9	325	35	40	55	60
$\% (D < 1 \mu\text{m})$	0	10	16	44	70	0	14	0	19	20	6	0
Luminescence intensity (relative scale)	100	105	120	103	98	124	111	100	92	102	116	150

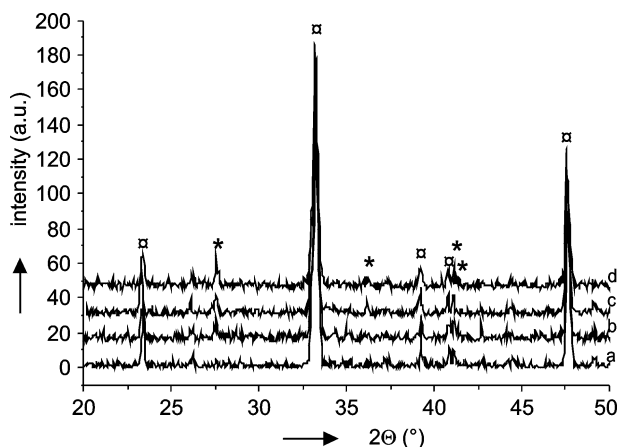


Figure 1. X-ray diffraction patterns of SS_{*i*} samples for different grinding times $t = 0$ min (a), $t = 15$ min (b), $t = 35$ min (c) and $t = 75$ min (d). * indicates TiO₂ (84-1284) and □ indicates CaTiO₃ (75-2100).

monomodal distribution of particles having an average size of about 200 μm. Under neutral conditions ($r = 0.78$), the average particle size is divided by a factor of around 10 and the distribution becomes bimodal with about 20 % of submicron particles. At least, as the basicity is further increased, ($r \gg 2$), the average particle size grows slightly and the distribution turns gradually from bimodal to monomodal, suggesting again re-aggregation of the smallest particles.

Scanning electron microscopy

SEM micrographs of SS_{*i*} and SG_{*r*} samples are shown in figure 3 and 4, respectively. In the case of SS_{*i*} powders, the microstructure consists of aggregates of micrometric or submicrometric grains, as can be observed and measured on enlarged views of the micrographs displayed on figure 3 (these views are not shown here). For unground SS₀, the sintering treatment at 1200 °C causes coalescence and aggregation of individual grains in a way such that it gives rise to some porosity. 15 to 35 minutes grinding (samples SS₁₅ and SS₃₅) provokes mainly the dissociation of the biggest aggregates, as indicated by a decrease of $D(0.9)$ and $D(av)$ values, thus contributing to release micrometric or submicrometric grains which can partially fill the pores and induce further densification of the microstructure. The comparison between SS₁₅ and sifted samples confirms that the microstructure appears less dense when the smallest particles are removed (ie in SS₁₅(>5 μm)) and confirms furthermore that these smallest particles tend to re-aggregate (in SS₁₅(<5 μm)). After 75 minutes grinding, the SEM micrograph shows that most of the grains have

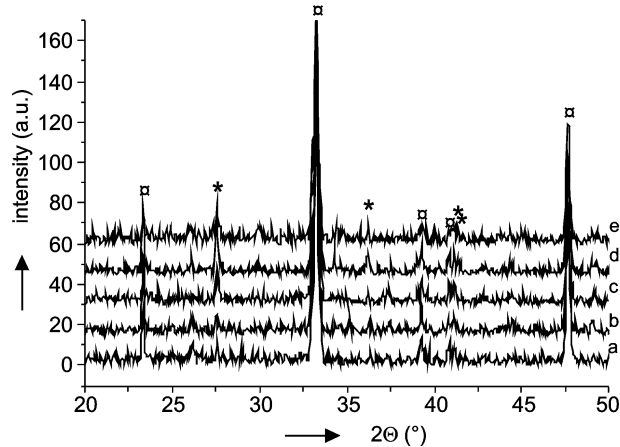


Figure 2. X-ray diffraction patterns of SG_{*r*} samples for different values of r : $r = 17$ (a), $r = 12.7$ (b), $r = 8.5$ (c) $r = 0.78$ (d) and $r = 0.39$ (e). * indicates TiO₂ (84-1284) and □ indicates CaTiO₃ (75-2100).

been broken, providing a quite narrow grain size distribution centered at around 2 μm, together with a large amount of submicron particles. The SG_{*r*} powders consists of rather dense aggregates whose size and microstructure depend strongly on the r value. For $r = 0.39$, the aggregates are made up of a dense and regular distribution of grains with sizes ranging from 0.7 to 3 μm in average. For $r = 0.78$, the average aggregates size is about 10 times smaller than for SG_{0.39} powder and the microstructure consists of a dense, almost equisized distribution of submicron grains. For $r > 8$, the microstructure is very different, since it consists of much larger grains (about 3 to 5 μm large in average) with a geometrical morphology, covered in places by submicron particles.

Luminescence

The luminescence intensity of the red emission of praseodymium in all the Pr³⁺-doped titanate powders SS_{*i*} and SG_{*r*} has been carefully analysed. The luminescence intensity of SS₀ and SG_{0.39} samples has been assigned arbitrarily to 100, making the comparison of emission intensities accurate only within the serials SS_{*i*} (as a function of t) and SG_{*r*} (as a function of r), respectively. For SS_{*i*} samples, the luminescence intensity increases up to $t = 15$ min and then decreases as t is further increased. This behaviour can be discussed by considering mainly structural and microstructural arguments. Accordingly, from SS₀ to SS₁₅, the improvement of the luminescence intensity can be accredited mainly to the enhancement of powder densification due to grinding, which contributes to increase the luminescence emitted

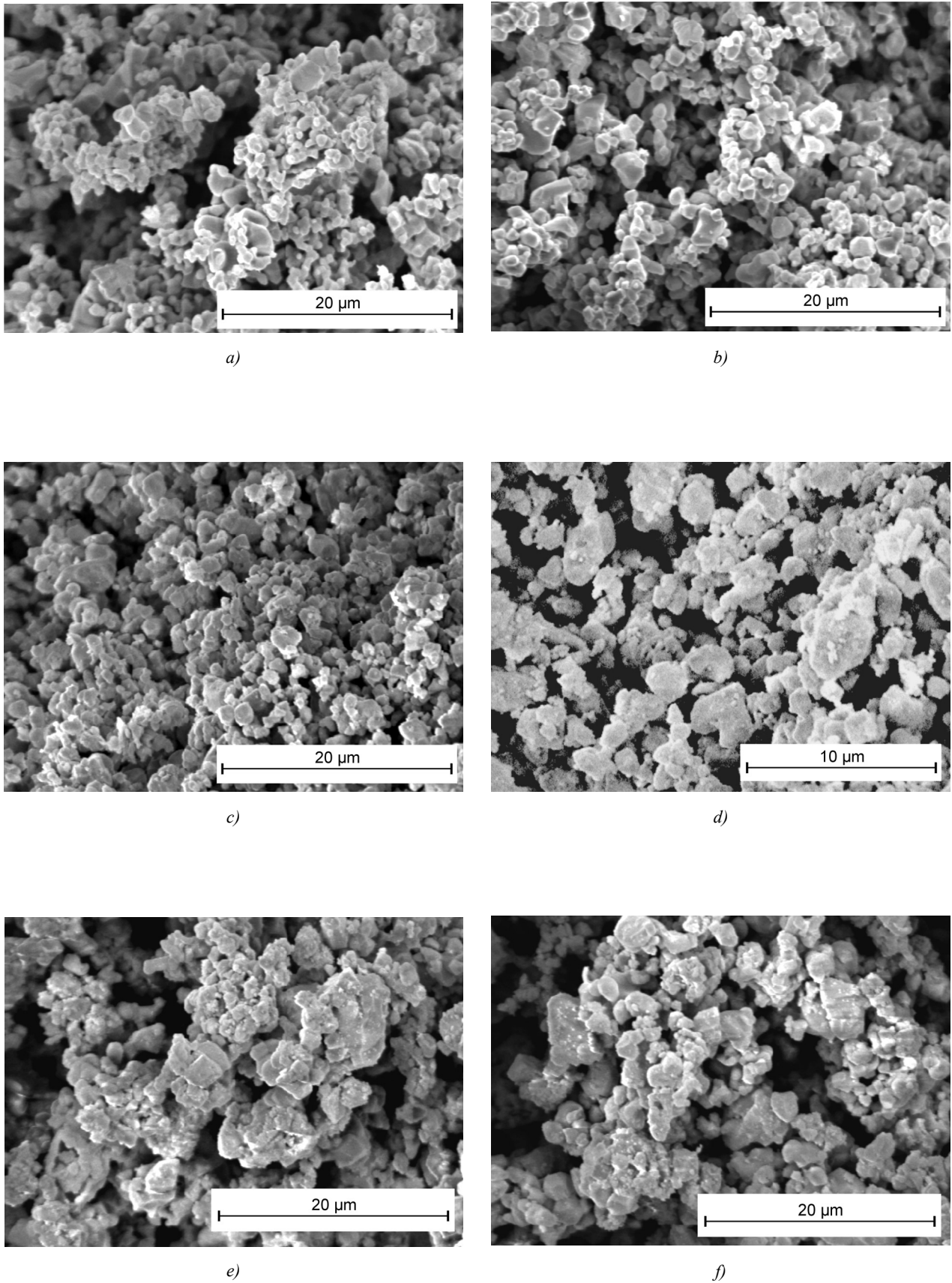


Figure 3. SEM micrographs of SS_0 (a), SS_{15} (b), SS_{35} (c), SS_{75} (d), $\text{SS}_{15} (>5\ \mu\text{m})$ (e) and $\text{SS}_{15} (<5\ \mu\text{m})$ (f).

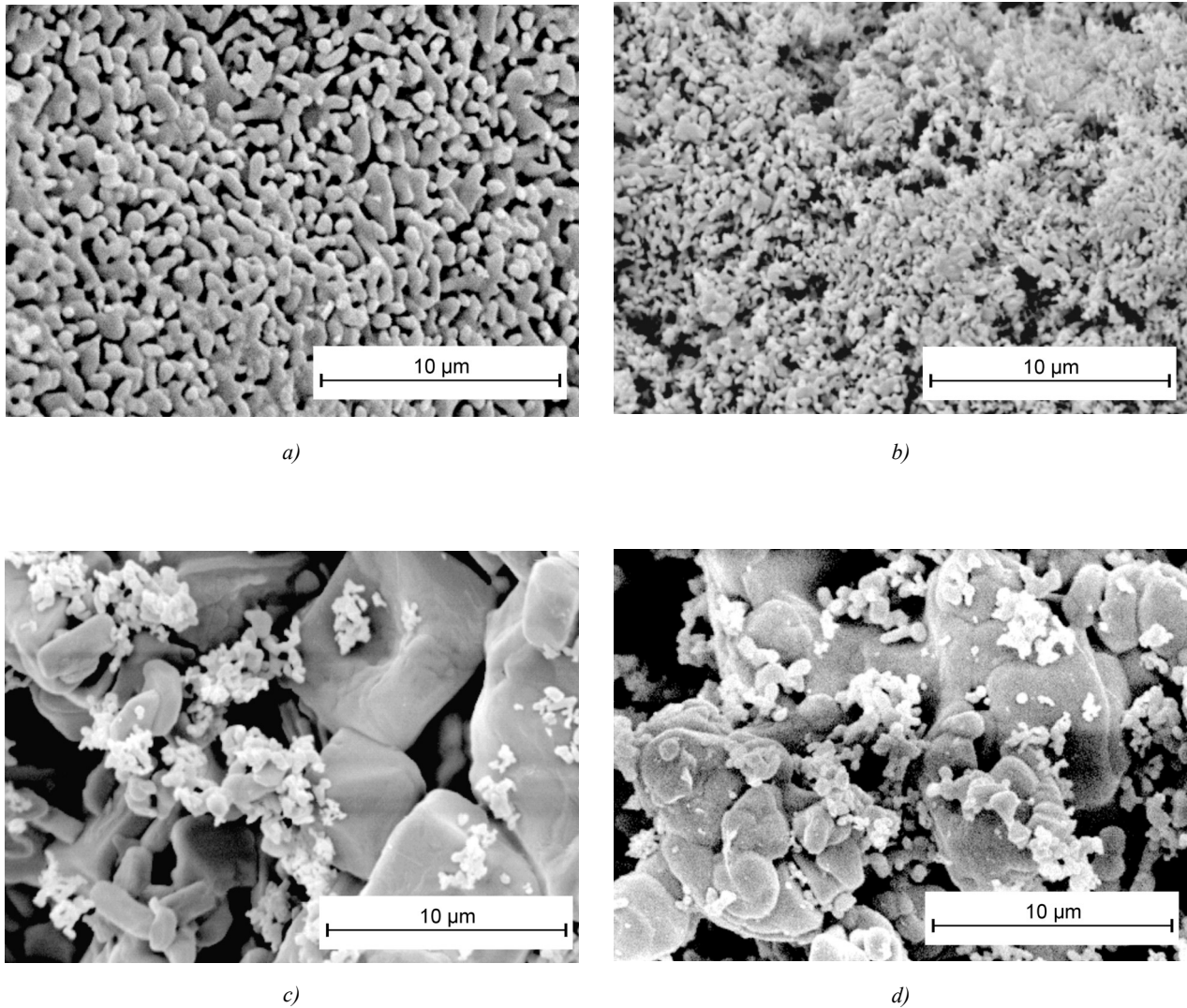


Figure 4. SEM micrographs of SG_{0.39} (a), SG_{0.78} (b), SG_{8.5} (c) and SG_{12.7} (d).

by surface unit of powder. This effect of densification is strong enough to compensate for the appearance of a small amount of non-luminescent rutile, as detected in the XRD pattern of SS₁₅. In contrast, the brightness of SS₃₅ is more than 14 % lower than SS₁₅ despite a microstructure as dense as the SS₁₅ one, a lower average grain size and a similar amount of rutile (see figure 1). Accordingly, it is assumed that the decrease of luminescence intensity in SS₃₅ can be induced by the increasing amount of submicron particles (see table 1) for which stronger light scattering processes can compete with absorption / emission processes. Such an assumption is corroborated by the comparison of SS₁₅ and corresponding sifted samples, since it is observed an improvement

of the luminescence intensity in the sample SS₁₅ (> 5 μm) containing no submicron particles and a decrease of the brightness in SS₁₅ (<5 μm). Similarly, the sample SS₇₅ exhibits the weakest luminescence intensity of the whole SS_i series, in spite of a narrow grain size distribution and a dense microstructure, which can again be interpreted as a consequence of an important proportion of submicron particles, together with a slight increase of the amount of non-luminescent rutile. Concerning SG_i samples, it is observed, as in the case of SS_i samples, that the luminescence intensity decreases in samples SG_{0.39} and SG_{0.78}, which present CaTiO₃ + TiO₂ phase mixing and for which the microstructure contains a large amount of submicron particles.

CONCLUSION

The microstructural and luminescence characteristics of solid state (SS) and sol-gel (SG) processed $\text{CaTiO}_3:\text{Pr}^{3+}$ powders have been investigated as a function of the grinding time t , in the case of SS_t samples and of the $\text{OH}/\text{Ti}(\text{OPr})_4$ molar ratios r , in the case of SG_r samples. It is observed that either a post-synthesis grinding time longer than 35 minutes or sol-gel syntheses operated under acidic or neutral conditions (without any grinding before or after firing at 1200 °C) lead to submicron microstructures, $\text{CaTiO}_3 + \text{TiO}_2$ phase mixing and to less efficient phosphors. The observed decrease of the luminescence intensity in both series of samples is then attributed to the presence of non-luminescent rutile and to the amount of submicrometric particles, for which stronger light scattering processes can compete with absorption / emission processes.

Acknowledgement

One of the authors (P. J.) acknowledges financial support by the ERASMUS program.

References

1. Shionoya S., Yen W.M.: *Phosphor Handbook*, CRC Press, Boca Raton 1999.
2. Chadha S.S., Smith D.W., Vecht A., C.S.: Gibbons, 94 SID Digest 51, 1 (1994).

3. Diallo P.T., Jeanlouis K., Boutinaud P., Mahiou R., Cousseins J.C.: *J.Alloys Compd.* 323-324, 218 (2001)
4. Chaput F., Boilot J.P.: *J.Mater.Sci.Lett.* 6, 1110 (1987).

VLIV MIKROSTRUKTURY NA INTENZITU LUMINISCENCE CaTiO_3 DOPOVANÉHO IONTY Pr^{3+}

P. BOUTINAUD, E. PINEL, G. BERTRAND AND R. MAHIOU,
P. JAKUBCOVÁ*, S. KASA*

*Laboratoire des Matériaux Inorganiques - UMR CNRS 6002.
Université Blaise-Pascal et ENSCCF
Ensemble Scientifique des Cèzeaux, 63177 Aubiere Cedex,
France*

**Ústav skla a keramiky,
Vysoká škola chemicko-technologická v Praze,
Technická 5, 166 28 Praha*

U vzorků prášků CaTiO_3 dopovaných ionty Pr^{3+} byla sledována závislost doby mletí (u vzorků připravených mechanickou cestou), resp. molárního poměru $\text{OH}/\text{Ti}(\text{OPr})_4$ (u vzorků připravených metodou sol-gel) na jejich mikrostrukturní a luminescenční charakteristice. Bylo pozorováno, že jak při delším mletí vzorku po syntéze, tak syntézy sol-gel provedené v kyselém nebo neutrálním prostředí, vedou k tvorbě submikronové mikrostruktury, k tvorbě smíšené fáze $\text{CaTiO}_3 + \text{TiO}_2$ a v důsledku toho k měni účinným luminoforům. Pozorované snížení intenzity luminescence je v souladu s přítomností rutilu ve vzorcích, který nemá luminescenční vlastnosti, a s množstvím submikronových částic ve vzorcích.